Neuron
Article

PAR-1 Kinase Phosphorylates Dlg and Regulates Its Postsynaptic Targeting at the *Drosophila* Neuromuscular Junction

Yali Zhang,[1] Huifu Guo,[3] Helen Kwan,[2] Ji-Wu Wang,[1] Jon Kosek,[2] and Bingwei Lu[1,*]
[1] Department of Pathology, Stanford University School of Medicine, GRECC/VAPAHCS, Palo Alto, CA 94304, USA
[2] Department of Pathology, Stanford University School of Medicine, Pathology Services/VAPAHCS, Palo Alto, CA 94304, USA
[3] Blanchette Rockefeller Neuroscience Institute, 9601 Medical Center Drive, Rockville, MD, 20852, USA
*Correspondence: bingwei@stanford.edu
DOI 10.1016/j.neuron.2006.12.016

SUMMARY

Targeting of synaptic molecules to their proper location is essential for synaptic differentiation and plasticity. PSD-95/Dlg proteins have been established as key components of the postsynapse. However, the molecular mechanisms regulating the synaptic targeting, assembly, and disassembly of PSD-95/Dlg are not well understood. Here we show that PAR-1 kinase, a conserved cell polarity regulator, is critically involved in controlling the postsynaptic localization of Dlg. PAR-1 is prominently localized at the *Drosophila* neuromuscular junction (NMJ). Loss of PAR-1 function leads to increased synapse formation and synaptic transmission, whereas overexpression of PAR-1 has the opposite effects. PAR-1 directly phosphorylates Dlg at a conserved site and negatively regulates its mobility and targeting to the postsynapse. The ability of a nonphosphorylatable Dlg to largely rescue PAR-1-induced synaptic defects supports the idea that Dlg is a major synaptic substrate of PAR-1. Control of Dlg synaptic targeting by PAR-1-mediated phosphorylation thus constitutes a critical event in synaptogenesis.

INTRODUCTION

Dynamic modulation of synaptic structure and function plays a fundamental role in the formation of neuronal networks during the development of the nervous system. It is also considered a molecular basis of learning and memory (Goda and Davis, 2003). Synapses are polarized structures that exhibit asymmetric distribution of proteins and RNAs. Rapid progress has been made in identifying structural components of the synapses. Dlg is a founding member of the membrane-associated guanylate kinase (MAGUK) family of synaptic proteins that contain PSD-95-Disc Large-Zonular Adhesion (PDZ), Src homology 3 (SH3), and GUK domains. Dlg was originally identified as a tumor suppressor in *Drosophila*, which, when mutated, causes tumor growth in the brain and imaginal discs of epithelial origin (Woods and Bryant, 1991). In epithelial cells and other cell types such as neuroblasts, Dlg plays a fundamental role in establishing cell polarity (Humbert et al., 2003). In the postsynaptic density of mammalian central synapses and *Drosophila* larval neuromuscular junction (NMJ), PSD-95/Dlg serves as a scaffold protein that recruits diverse synaptic proteins and assembles them into large protein complexes (Funke et al., 2005; Kennedy and Ehlers, 2006; Kim and Sheng, 2004; Koh et al., 2000). Synaptic proteins that are regulated by PSD-95/Dlg include Shaker type K^+ channels, glutamate receptors, synaptic cell adhesion molecules, cytoskeletal proteins, and other signaling proteins such as neuronal NO synthase. The assembly processes orchestrated by PSD-95/Dlg are critical events in synaptic differentiation and maturation (Kim and Sheng, 2004). However, the molecular mechanisms that regulate the abundance, localization, and activity of PSD-95/Dlg during synapse formation or other cell polarization processes are not well understood.

The PAR genes (PAR-1 through PAR-6) were identified in a genetic screen for genes that control asymmetric cell division during *C. elegans* early embryogenesis (Kemphues et al., 1988). PAR-1 encodes a conserved Ser/Thr kinase that plays critical roles in regulating cell polarity in diverse cell types and organisms (Guo and Kemphues, 1995). In *Drosophila* and mammals, PAR-1 and its homolog, MARK, have been implicated in the polarization of oocytes, epithelial cells, and neurons (Biernat et al., 2002; Shulman et al., 2000; Tomancak et al., 2000). The first clue about the molecular function of PAR-1-like kinases came from studies of MARK, a kinase that phosphorylates the microtubule (MT) binding protein tau (Drewes et al., 1997), whose abnormal phosphorylation has been observed in neurodegenerative diseases (Augustinack et al., 2002). In *Drosophila*, PAR-1 acts as a physiological tau kinase and its aberrant activation can lead to neurodegeneration (Nishimura et al., 2004). These studies therefore implicate aberrant activation of PAR-1 in the pathogenesis of Alzheimer's disease (AD) and related

tauopathies. Importantly, PAR-1 overexpression leads to a stronger neurodegenerative phenotype than tau overexpression, suggesting that other substrates may also mediate PAR-1-induced toxicity. Given the close link between synaptic failure and neurodegenerative diseases (Selkoe, 2002), and given the involvement of cell polarity regulators in synapse development, the following questions are raised: does PAR-1 normally play a role at the synapse? If so, which synaptic protein or proteins are the direct target?

Here we show that PAR-1 and Dlg, two important cell polarity regulators, functionally interact at the synapse to control synaptic development and function and that Dlg is a direct target of PAR-1 at the *Drosophila* NMJ. We find that PAR-1 protein is enriched at the postsynapse of the *Drosophila* NMJ. In both loss-of-function and gain-of-function studies, we find that the precise level of PAR-1 activity is critical for synaptic differentiation and function. Furthermore, the synaptic targeting of Dlg is tightly controlled by PAR-1. We provide evidence that PAR-1 regulates Dlg synaptic targeting through phosphorylation at a conserved S797 site. Our morphological and functional rescue studies clearly show that Dlg is a key downstream target through which PAR-1 influences synaptic development and function.

RESULTS

Localization of PAR-1 at the *Drosophila* NMJ

As an initial step toward studying the synaptic function of PAR-1, we examined the localization patterns of PAR-1 at the *Drosophila* larval NMJ, using a polyclonal antibody raised against a nonconserved region of *Drosophila* PAR-1 protein (Sun et al., 2001). PAR-1 immunoreactivity was clearly present at the NMJ. Prominent anti-PAR-1 signals were found at the type I boutons (Figure 1A1), an excitatory glutamatergic synapse (Jan and Jan, 1976). Relatively weaker anti-PAR-1 signals were also detected in the muscle cytoplasm. To confirm the specificity of PAR-1 antibody staining, similar experiments were performed in *par-1* mutant animals. Since a putative *par-1* null mutant ($par\text{-}1^{\Delta 416}$) is homozygous lethal at late embryonic stages (Sun et al., 2001), we generated heteroallelic mutants in which $par\text{-}1^{\Delta 416}$ was placed in *trans* to a well-characterized viable allele $par\text{-}1^{9A}$ (Tomancak et al., 2000). A small percentage of $par\text{-}1^{\Delta 416}/par\text{-}1^{9A}$ mutant (referred to as *par-1* mutant) animals can survive to late larval stages, allowing us to carry out structural and functional analysis. As shown in Figure 1B1, anti-PAR-1 signals were dramatically decreased in both the synaptic and extrasynaptic regions in *par-1* mutant NMJ. Western blot analysis also showed that PAR-1 protein levels were dramatically reduced in *par-1* mutant NMJ (see Figure S1 in the Supplemental Data). These experiments thus confirmed the expression of PAR-1 at the larval NMJ.

To precisely determine the synaptic localization of PAR-1 at the NMJ, we performed double-labeling experiments using antibodies against presynaptic markers, such as HRP (Jan and Jan, 1982) and CSP (Zinsmaier et al., 1994), and a postsynaptic marker Dlg (Parnas et al., 2001). Anti-PAR-1 signals largely overlapped with anti-Dlg (Figures 1A1–1A3 and 1D), but were mostly nonoverlapping with either anti-HRP (Figures 1C1–1C3 and 1E) or anti-CSP (Figure 1F). Only a small portion of anti-PAR-1 signals was observed in the presynapse. Furthermore, a PAR-1-GFP fusion protein was also preferentially localized to the postsynaptic region when ectopically expressed in the muscle cells (Figure S2). These results indicate that PAR-1 localization is enriched at the postsynaptic region of the *Drosophila* NMJ.

Loss of Function and Overexpression of PAR-1 Cause Defects in Synaptic Morphogenesis

To assess the potential role of PAR-1 kinase at the synapse, we carried out anatomical analysis of *par-1* mutant NMJs. We used the anti-HRP antibody to examine the motor neuron nerve terminal profile and synaptic bouton morphology. Compared with the controls, *par-1* mutants manifested a mild increase in synapse formation. In wild-type animals, motor neuron nerve terminals innervating muscle 6/7 form type I boutons, which are big and spherical (Figure 1G). However, irregularly shaped boutons were frequently observed on muscle 6/7 in *par-1* mutant animals (Figure 1H). The sizes of these boutons were noticeably smaller (control: $8.2 \pm 0.4\ \mu m^2$, $n = 20$; *par-1* mutant: $4.0 \pm 0.3\ \mu m^2$, $n = 27$; $p < 0.01$). The number of boutons formed on muscle 6/7 exhibited a mild but statistically significant increase (Figure 1H and Figure 2E). Similar results were observed in $par\text{-}1^{9A}/par\text{-}1^{W3}$ heteroallelic animals (data not shown).

Since complete loss of PAR-1 is pleiotropic and causes embryonic lethality, we sought to use a complementary approach to assess PAR-1 loss-of-function effect at the synapse. For this purpose, we generated *PAR-1 RNAi* flies. With the *UAS/Gal4* system, we selectively knocked down PAR-1 expression at the postsynapse or presynapse using the muscle-specific driver *Mhc-Gal4* (Davis et al., 1997) or the neuron-specific driver *elav-Gal4* (Lin and Goodman, 1994), respectively. Immunostaining and western blot analyses confirmed that PAR-1 protein level was dramatically reduced in body-wall muscle extract of *Mhc>PAR-1 RNAi* animals (Figures S1 and S3). *Mhc>PAR-1 RNAi* animals also exhibited smaller-sized boutons (control: $8.2 \pm 0.4\ \mu m^2$, $n = 20$; *Mhc>PAR-1 RNAi*: $4.2 \pm 0.2\ \mu m^2$, $n = 24$; $p < 0.01$). There was also a mild increase in bouton number in these animals (Figure 1I and Figure 2E). In contrast, presynaptic knockdown of PAR-1 in *elav>PAR-1 RNAi* animals had no significant effect on synapse formation (Figure 2E).

We then examined the effect of PAR-1 overexpression on synapse development using a *UAS-PAR-1* transgene (Sun et al., 2001). As a control, we used a transgene expressing a kinase-dead form of PAR-1 (PAR-1 KD). PAR-1 KD is generally considered inactive (Nishimura et al., 2004). However, in certain settings, PAR-1 KD or MARK KD exerts dominant-negative effects when

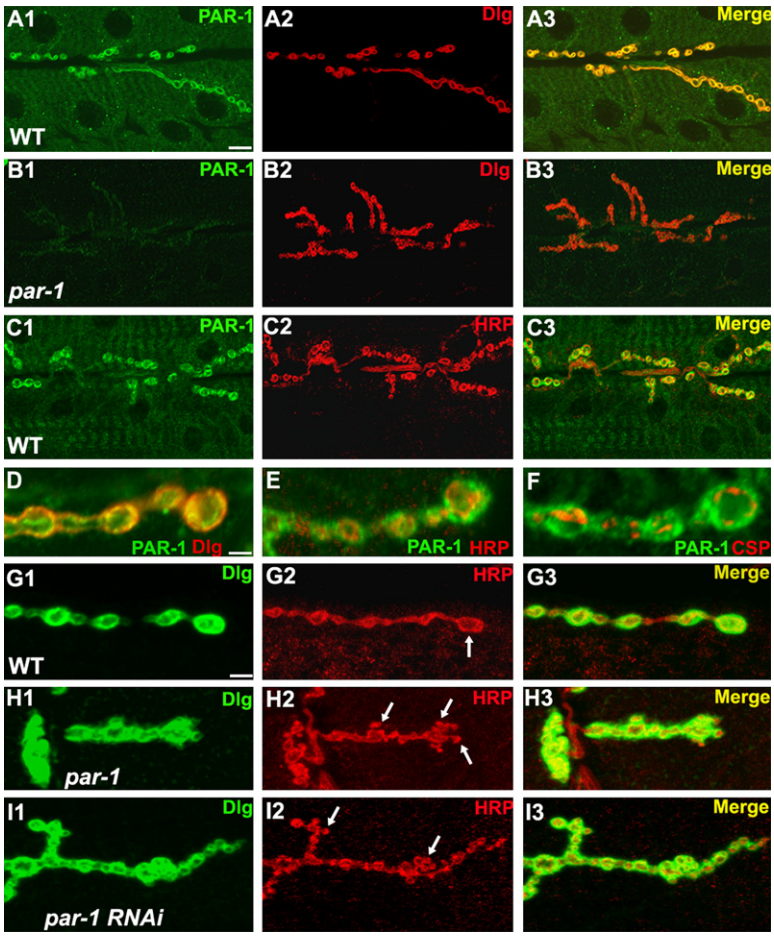

Figure 1. Expression and Function of PAR-1 at the Larval NMJ

(A1–A3) Immunostaining of wild-type third-instar larval NMJs with anti-PAR-1 (A1) and anti-Dlg (A2) antibodies. The merged image is shown in (A3). Scale bar in (A1), 5 μm.

(B1–B3) Immunostaining of *par-1*$^{\Delta 416}$/*par-1*^{9A} mutant third-instar larval NMJ with anti-PAR-1 (B1) and anti-Dlg (B2) antibodies. The merged image is shown in (B3). Note that in *par-1* mutant NMJs, there is a marked decrease in anti-PAR-1 signals.

(C1–C3) Immunostaining of wild-type third-instar larval NMJs with anti-PAR-1 (C1) and anti-HRP (C2) antibodies. The merged image is shown in (C3).

(D–F) Higher magnification views of wild-type boutons double-labeled with PAR-1 (green)/Dlg (red) in (D), PAR-1 (green)/HRP (red) in (E), or PAR-1 (green)/CSP (red) in (F). Scale bar in (D), 1 μm.

(G1–I3) Comparison of synapse morphology in wild-type and PAR-1 loss-of-function animals. In wild-type (G1–G3), the type I boutons appear as big and spherical structures (arrow) outlined by anti-Dlg (G1) and anti-HRP (G2). In *par-1*/*par-1*^{9A} mutants (H1–H3) and *Mhc>PAR-1 RNAi* animals (I1–I3), some boutons appear smaller and irregularly shaped (arrows). There is no obvious difference in overall Dlg localization pattern between wild-type and *par-1* mutant, although the intensity of anti-Dlg signal at the synaptic region appears mildly increased. However, in both *par-1* mutant and *Mhc>PAR-1 RNAi*, the anti-Dlg intensities at the synaptic region are mildly enhanced. Scale bar in (G1), 2 μm.

overexpressed (Biernat et al., 2002; Sun et al., 2001). Wild-type PAR-1 or PAR-1 KD was expressed postsynapticaly or presynaptically using *Mhc-Gal4* or *elav-Gal4*, respectively. Strikingly, postsynaptic, but not presynaptic, overexpression of PAR-1 caused severe defects in synapse development. At muscle 6/7, there was an estimated 60% decrease in the total number of type I boutons, and the structure of synaptic nerve terminals was oversimplified (Figures 2A2 and 2E). Overall bouton number and branching complexity in *Mhc>PAR-1 KD* animals were not significantly different from the controls (Figure 2C2). Collectively, these results indicate that postsynaptic PAR-1 imposes a constraint on synapse development and that the precise level of PAR-1 activity is critical for establishing and maintaining synaptic structures.

PAR-1 Regulates the Postsynaptic Targeting of Dlg

To explore the mechanism by which PAR-1 operates at the postsynapse to govern synapse differentiation and function, we attempted to identify the synaptic targets of PAR-1. As our initial studies showed that PAR-1 and Dlg colocalize at the postsynapse (Figures 1A3 and 1D), Dlg represents a candidate target. We therefore examined the effect of PAR-1 on Dlg localization. In control animals, Dlg was specifically targeted to the postsynapse (Figures 2B1–2B3). However, the postsynaptic targeting of Dlg was severely disrupted in *Mhc>PAR-1* animals. Dlg signal was scattered throughout the muscle cell. At the postsynapse, Dlg signal was diffuse and less concentrated (Figures 2A1–2A3). Quantitative analysis revealed an ~50% decrease of synaptic Dlg level and a concomitant ~3-fold increase of Dlg level in the extrasynaptic region (Figure 2F). We also examined Dlg localization in *par-1* mutant or *PAR-1 RNAi* animals. Dlg was restricted to the postsynapse in *par-1* mutants or *PAR-1 RNAi* animals (Figures 1H1 and 1I1). However, the ratio of synaptic versus extrasynaptic Dlg levels was moderately higher than that in control animals, suggesting that loss of PAR-1 enhanced Dlg synaptic targeting (Figure 2F). Likewise, in *Mhc>PAR-1 KD* animals, Dlg was also restricted to the postsynapse, and the ratio of synaptic versus extrasynaptic Dlg levels was higher than that in the controls (Figures 2C and 2F), suggesting that in terms of Dlg postsynaptic targeting, overexpressed PAR-1 KD might exert dominant-negative effects on endogenous PAR-1 function.

To further confirm that PAR-1 overexpression-induced synaptic phenotypes reflect the normal activity of endogenous PAR-1, we examined the effect of reducing endogenous PAR-1 function on PAR-1 overexpression phenotypes. When endogenous PAR-1 activity was reduced in

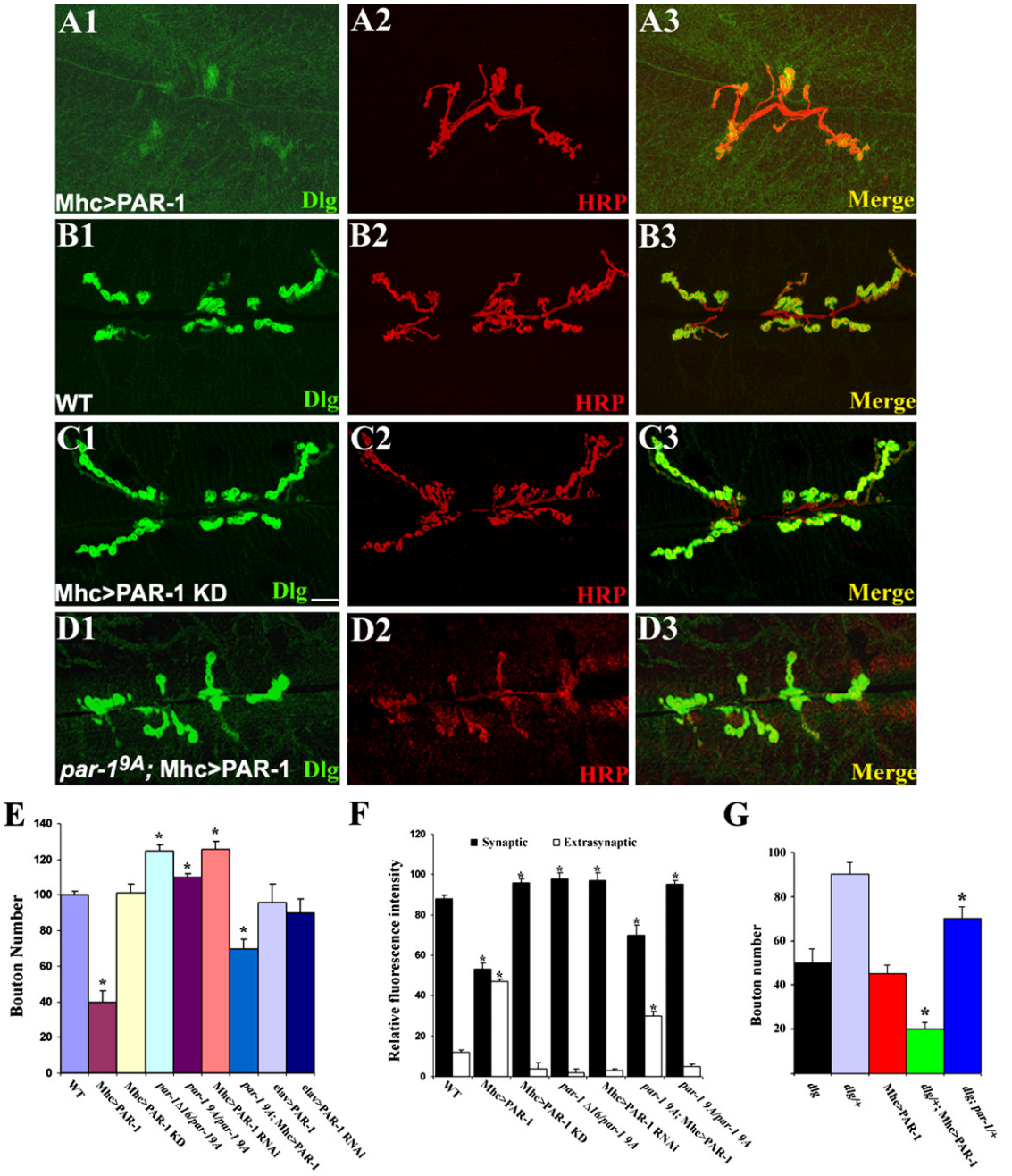

Figure 2. PAR-1 Regulates the Postsynaptic Synaptic Targeting of Dlg and Synapse Development

(A1–D3) Immunostaining of larval NMJs in control and transgenic animals expressing PAR-1 or PAR-1 KD postsynaptically. The genotypes are: *Mhc>PAR-1* (A1–A3), *Mhc-Gal4/+* (B1–B3), *Mhc>PAR-1 KD* (C1–C3), and *par-1^{9A}*; *Mhc>PAR-1* (D1–D3). NMJs were double-labeled with anti-Dlg (green) and anti-HRP (red). Scale bar, 5 μm.

(E) A bar graph showing statistical analysis of bouton number in PAR-1 loss-of-function and overexpression animals. Wild-type (n = 30); *Mhc>PAR-1* (n = 35); *Mhc>PAR-1 KD* (n = 29); *elav>PAR-1* (n = 25); *par-1$^{\Delta 16}$/par-1^{9A}* mutant (n = 32); *par-1^{9A}/par-1^{9A}* mutant (n = 28); *par-1^{9A}*; *Mhc>PAR-1* (n = 26); *Mhc>PAR-1 RNAi* (n = 26), and *elav>PAR-1 RNAi* (n = 20) genotypes were analyzed. The differences between wild-type and *Mhc>PAR-1* ($p < 0.001$) and between wild-type and *par-1$^{\Delta 16}$/par-1^{9A}* mutants ($p < 0.01$), *par-1^{9A}/par-1^{9A}* mutant ($p < 0.05$), and *Mhc>PAR-1 RNAi* ($p < 0.01$) are statistically significant in Student's t test. The difference between *Mhc>PAR-1* and *par-1^{9A}*; *Mhc>PAR-1* is also statistically significant ($p < 0.01$).

(F) Quantitative measurements of relative anti-Dlg fluorescence intensity between the synaptic and extrasynaptic regions in wild-type (n = 30), *Mhc>PAR-1* (n = 35), *Mhc>PAR-1 KD* (n = 25), *par-1$^{\Delta 16}$/par-1^{9A}* mutant (n = 32), *Mhc>PAR-1 RNAi* (n = 26), *par-1^{9A}*; *Mhc>PAR-1* (n = 26), and *par-1^{9A}/par-1^{9A}* mutant (n = 28) animals. The differences between wild-type and *Mhc>UAS-PAR-1* ($p < 0.001$) and between wild-type and *Mhc>PAR-1 KD* ($p < 0.01$), *par-1$^{\Delta 16}$/par-1^{9A}* mutants ($p < 0.01$), *par-1^{9A}/par-1^{9A}* mutants ($p < 0.01$), or *Mhc>PAR-1 RNAi* ($p < 0.01$) are statistically significant. The difference between *Mhc>PAR-1* and *par-1^{9A}*; *Mhc>PAR-1* is also statistically significant ($p < 0.01$).

a *par-1*^{9A} mutant background, the deleterious effect of PAR-1 overexpression on synapse formation was moderately attenuated (Figures 2D and 2E), suggesting that the PAR-1 overexpression phenotype was dosage-dependent and that endogenous PAR-1 also contributed to the effect. We found that Dlg protein levels among wild-type, *Mhc>PAR-1*, and *Mhc>PAR-1 KD* animals were comparable (Figure S4), suggesting that PAR-1 overexpression had no obvious effect on the turnover of Dlg protein. Together, the loss-of-function and overexpression results support the notion that PAR-1 negatively regulates the synaptic targeting of Dlg.

One possible cause of Dlg delocalization in *Mhc>PAR-1* animals might be a developmental defect of the muscle. Two observations argue against this. First, *Mhc>PAR-1* animals had normal muscle fiber number, organization, and muscle sizes (Figure S5). Second, we examined the distribution patterns of glutamate receptor II subunit A (GluRIIA) (DiAntonio et al., 1999), another postsynaptic marker. Although there was a mild decrease of GluRIIA levels at the postsynapse of *Mhc>PAR-1* animals compared with those of controls (Figure S6), unlike Dlg, GluRIIA was not delocalized and no increase in extrasynaptic GluRIIA was detected, indicating that GluRIIA was still preferentially targeted to the postsynapse. These results suggest that PAR-1 differentially regulates the postsynaptic targeting and abundance of Dlg and GluRIIA. The mechanism by which PAR-1 affects the abundance of GluRIIA is unknown.

Given the tight correlation between PAR-1 activity and Dlg synaptic localization, we next tested the genetic relationship between *par-1* and *dlg* in synapse development. In a severe *dlg* semilethal mutant, *dlg*$^{X1-2}$, loss of Dlg leads to a significant decrease of bouton number and simplification of synapse morphology (Figure 2G and Figure S7). In a PAR-1 overexpression background, removal of one copy of *dlg* exacerbated the synapse formation defects (Figure 2G and Figure S7), while homo- or hemizygosity of *dlg* resulted in complete larval lethality. Conversely, removal of one copy of *par-1* moderately ameliorated the synapse formation defects of the *dlg*$^{X1-2}$ mutant, as observed in *dlg*$^{X1-2}$*; par-1*$^{\Delta 416}$/+ animals (Figure 2G and Figure S7). Reduction of PAR-1 kinase activity might have allowed the residual Dlg activity in this mutant (provided by maternal wild-type Dlg [DlgWT] protein plus mutant Dlg) to function more effectively in promoting synaptic development. Dlg and PAR-1 therefore genetically interact to fine-tune synapse development.

PAR-1 Phosphorylates Dlg In Vitro and In Vivo

We have shown that the precise level of PAR-1 kinase activity is critical for normal Dlg localization and synaptic development. PAR-1/MARK kinase phosphorylates substrates containing KXGS motifs (Drewes et al., 1997; Nishimura et al., 2004). A putative phosphorylation site (S797) that matches the KXGS motif is present in Dlg GUK domain, a domain previously shown to direct Dlg synaptic targeting (Thomas et al., 2000). The S797 site is conserved in all MAGUK proteins of the PSD-95/Dlg family (Figure S8A). This raised the possibility that PAR-1 might

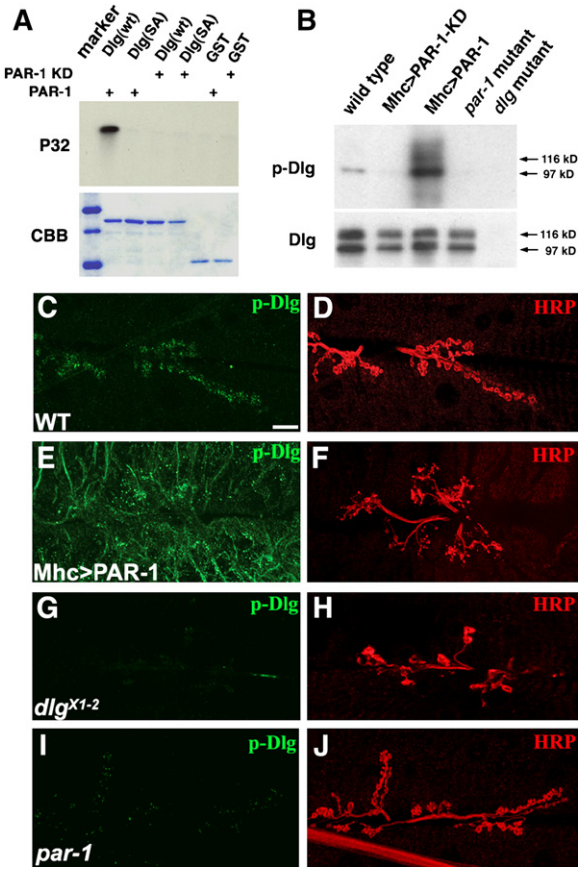

Figure 3. PAR-1 Phosphorylates Dlg In Vitro and In Vivo

(A) In vitro kinase assays showing phosphorylation of wild-type GST-Dlg fusion, but not GST-DlgSA, mutant proteins by PAR-1 kinase. Top, autoradiography; bottom, commassie blue (CBB) staining as control for protein loading.

(B) Western blot analysis showing in vivo phosphorylation of Dlg. Dlg proteins immunoprecipitated from larval body-wall muscle extracts of wild-type, *Mhc>PAR-1 KD, Mhc>PAR-1, par-1*$^{\Delta 416}$*/par-1*^{9A} mutant, and *dlg*$^{X1-2}$ mutant were probed with anti-p-Dlg antibody. Note that two isoforms of Dlg, 97 kDa and 116 kDa bands, possibly representing S97 and S97N (Mendoza et al., 2003), respectively, were present in body-wall muscle extracts, but the 97 kDa band showed preferential binding by anti-p-Dlg.

(C–J) Double-labeling of wild-type (C and D), *Mhc>PAR-1* (E and F), *dlg*$^{X1-2}$ mutant (G and H), and *par-1*$^{\Delta 416}$*/par-1*^{9A} mutant (G and H) larval NMJs with anti-p-Dlg (C, E, G, and I) and anti-HRP (D, F, H, and J). Scale bar in (C), 5 μm.

(G) Genetic interaction between *par-1* and *dlg*. The bouton-loss phenotype in *Mhc>PAR-1* (n = 35) was enhanced by removing one copy of *dlg* in *dlg*$^{X1-2}$*/+; Mhc-PAR-1* (n = 32, p < 0.001). In *dlg*$^{X1-2}$*; par-1*$^{\Delta 416}$/+ animals (n = 25), in which one copy of *par-1* was from a *dlg*$^{X1-2}$ mutant background, there was a partial suppression of the bouton-loss phenotype of *dlg*$^{X1-2}$ mutant (n = 22, p < 0.01).

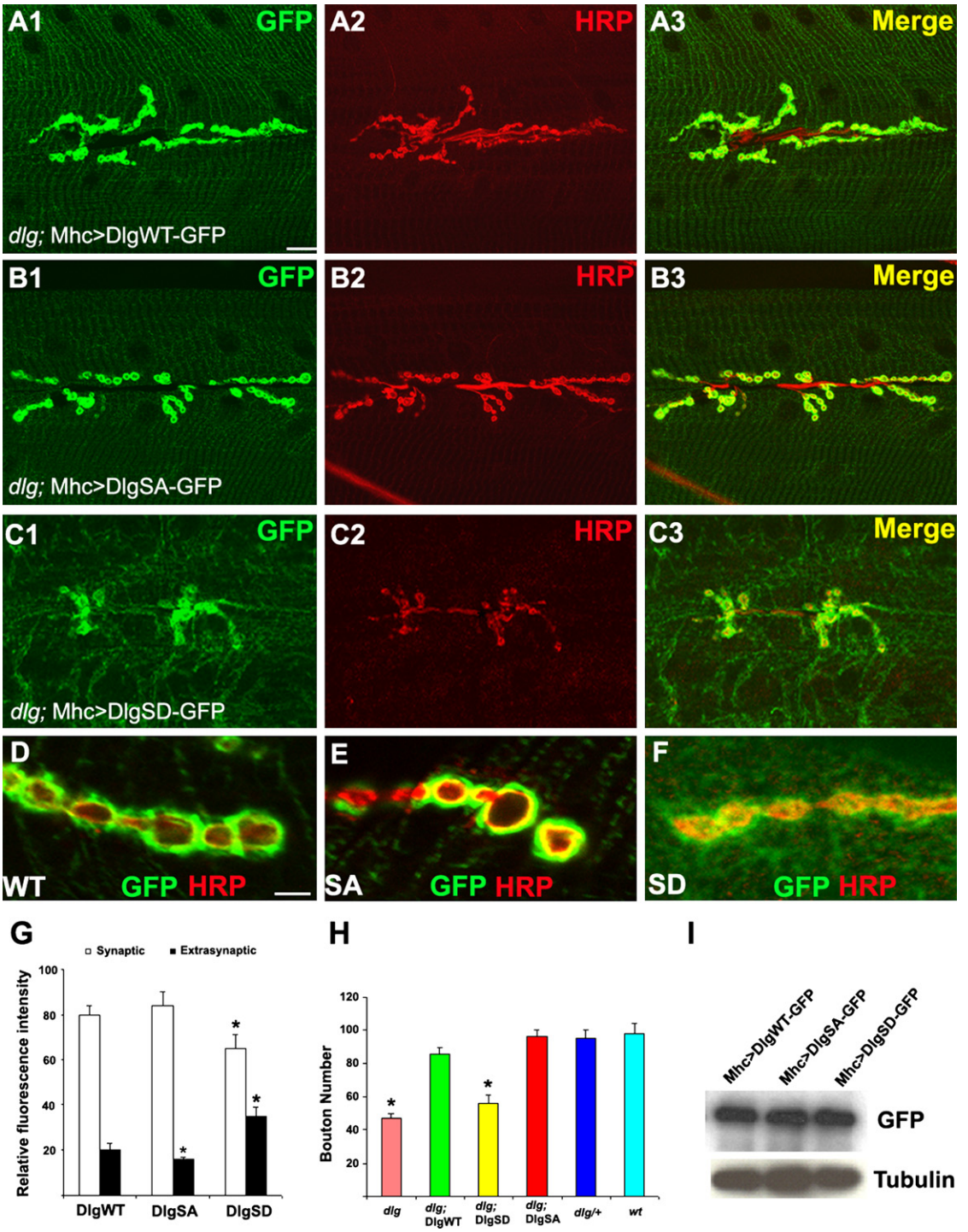

Figure 4. Analysis of the Synaptic Targeting Behavior of the Nonphosphorylatable DlgSA-GFP and Phospho-Mimetic DlgSD-GFP at the NMJ

(A1–C3) Labeling of DlgWT-GFP (A1–A3), DlgSA-GFP (B1–B3), and DlgSD-GFP (C1–C3) fusion proteins expressed postsynaptically in a dlg^{X1-2} mutant background. Exogenous Dlg-GFP fusions were detected by anti-GFP (green) and boutons were labeled with anti-HRP (red). Scale bar in (A1), 5 μm.

(D–F) High-magnification views of the distribution patterns of Dlg-GFP fusion variants. Scale bar in (D1), 1 μm.

(G) Quantification of relative distribution of the Dlg-GFP variants between the synaptic and extrasynaptic regions. The difference between DlgWT-GFP (n = 30) and DlgSD-GFP (n = 33) is significant ($p < 0.01$). The difference in the level of extrasynaptic GFP signal between DlgWT-GFP and DlgSA-GFP (n = 25) is also significant ($p < 0.05$).

directly phosphorylate Dlg at S797 to regulate its synaptic targeting and function.

To test whether PAR-1 phosphorylates Dlg S797, we performed in vitro kinase assays using affinity purified PAR-1 as the kinase source. GST fusion proteins of DlgWT GUK domain or mutant GUK in which S797 was mutated to Ala (GUK-SA) were used as substrates. As shown in Figure 3A, ^{32}P was incorporated into GST-GUK after the fusion protein was incubated with wild-type PAR-1, but not with PAR-1 KD. No ^{32}P incorporation was observed for GST-GUK-SA or GST protein alone. We conclude that PAR-1 can phosphorylate Dlg GUK domain in vitro at S797.

To investigate whether S797 is normally phosphorylated in vivo, we generated a phospho-S797-specific Dlg antibody. A heterologous cell line, HEK 293T, was used to test the specificity of the antibody. Cotransfection of DlgWT, but not Dlg S797 mutated to Ala (DlgS797A), together with wild-type PAR-1 into HEK 293T cells, resulted in robust phosphorylation of Dlg at S797. No Dlg phosphorylation was observed in cells cotransfected with PAR-1 KD and DlgWT, or in cells transfected with PAR-1 or Dlg alone (Figure S8B). The specificity of the phospho-Dlg (p-Dlg) antibody was further demonstrated by its preferential recognition of DlgWT over DlgS797A expressed in transgenic animals (Figure S8C).

We next used this p-Dlg antibody to analyze Dlg phosphorylation in vivo. Postsynaptic overexpression of wild-type PAR-1, but not PAR-1 KD, led to a robust induction of p-Dlg levels as shown by western blot and immunofluorescence analyses (Figures 3B and 3E). In *Mhc>PAR-1* animals, p-Dlg was broadly distributed in a manner similar to that of DlgS797D mutant-(DlgSD-) GFP (Figure 3E). A basal level of p-Dlg was detected in wild-type animals (Figures 3B and 3C), but no p-Dlg was detected in dlg^{X1-2} mutant (Figures 3B and 3G). In *par-1* mutant, the basal phosphorylation of Dlg was dramatically reduced in immunohistochemical analysis and undetectable on western blot (Figures 3B and 3I). These in vitro and in vivo results demonstrate that the S797 site in Dlg is a physiological site for PAR-1 kinase.

Phospho-Mimetic DlgSD-GFP Is Delocalized from the Synapse, whereas Nonphosphorylatable DlgSA-GFP Is Targeted Efficiently to the Synapse

To evaluate the role of PAR-1-mediated S797 phosphorylation in regulating Dlg synaptic targeting in intact animals, we generated transgenic flies expressing GFP-tagged Dlg constructs in which S797 was converted into Ala or Asp residues, making Dlg nonphosphorylatable or phosphomimetic, respectively. To compare the postsynaptic targeting of DlgWT, DlgS797A mutant (DlgSA), and DlgSD, the corresponding transgenes were expressed postsynaptically in a dlg^{X1-2} mutant background. DlgWT-GFP fusion proteins were almost all recruited to the synapse (Figures 4A1 and 4D). DlgSA-GFP was also concentrated at the synapse (Figures 4B1 and 4E). Quantification of relative fluorescence intensity in synaptic and extrasynaptic regions revealed that DlgSA-GFP was localized more efficiently to the synapse than DlgWT-GFP (Figure 4G). In contrast, DlgSD-GFP was partially delocalized from the synapse. Even though some portion of DlgSD-GFP could still accumulate around the synapse, its synaptic localization appeared less concentrated than DlgWT-GFP or DlgSA-GFP (Figures 4C1 and 4F).

We also evaluated the synaptic function of the different Dlg variants by testing their abilities to rescue the mutant phenotype of dlg^{X1-2}. DlgWT-GFP and DlgSA-GFP efficiently rescued the synapse-loss phenotype, whereas DlgSD-GFP failed to do so (Figure 4H). DlgWT-GFP and DlgSA-GFP, but not DlgSD-GFP, could also rescue the synaptic transmission defects of dlg^{X1-2} mutant (Figure S11). Thus, DlgWT and DlgSA, but not DlgSD, are functionally equivalent to endogenous Dlg. The differential rescuing ability of the Dlg variants was not due to unequal levels of transgene expression, since comparable levels of GFP fusion proteins were produced (Figure 4I). These in vivo studies confirm that the S797 site is important for Dlg function and that phosphorylation at this site negatively regulates the synaptic targeting of Dlg.

Fluorescent Recovery after Photobleaching Analysis Reveals a Faster Recovery of DlgSA-GFP at the Synapse, whereas the Recovery of DlgSD-GFP Is Slower

To characterize the effect of PAR-1-mediated phosphorylation on the dynamics of Dlg synaptic targeting in live animals, we used the fluorescent recovery after photobleaching (FRAP) approach to monitor Dlg-GFP movement at the NMJ. To collect stable and continuous confocal images from live animals, third-instar larvae were transiently immobilized by a pulse exposure to ether, a method previously used for in vivo imaging of NMJ synapse development (Rasse et al., 2005; Zito et al., 1999). The NMJs of abdominal muscle 12, one of the muscles closest to the transparent cuticle, were chosen for FRAP manipulation. We chose the distal synapses for FRAP analysis because they represent nascent synapses undergoing vigorous recruitment of newly synthesized molecules to expand and build new synapses at the larval stages (Lnenicka and Keshishian, 2000). Transgenes expressing similar levels of DlgWT-GFP, DlgSA-GFP, or DlgSD-GFP were expressed in a dlg^{X1-2} mutant background to exclude possible interference by endogenous Dlg protein. For DlgWT-GFP, after the bleaching of GFP

(H) Rescue of the synaptic formation defects of dlg^{X1-2} mutants by DlgSA- and DlgWT-, but not DlgSD-, GFP. The differences between wild-type ($n = 30$) and dlg^{X1-2} mutant ($n = 28$, $p < 0.01$) and between wild-type and dlg^{X1-2}; *DlgSD-GFP* ($n = 35$, $p < 0.01$) are statistically significant.
(I) Western blot analysis showing expression levels of the Dlg-GFP variants. Tubulin served as loading control.

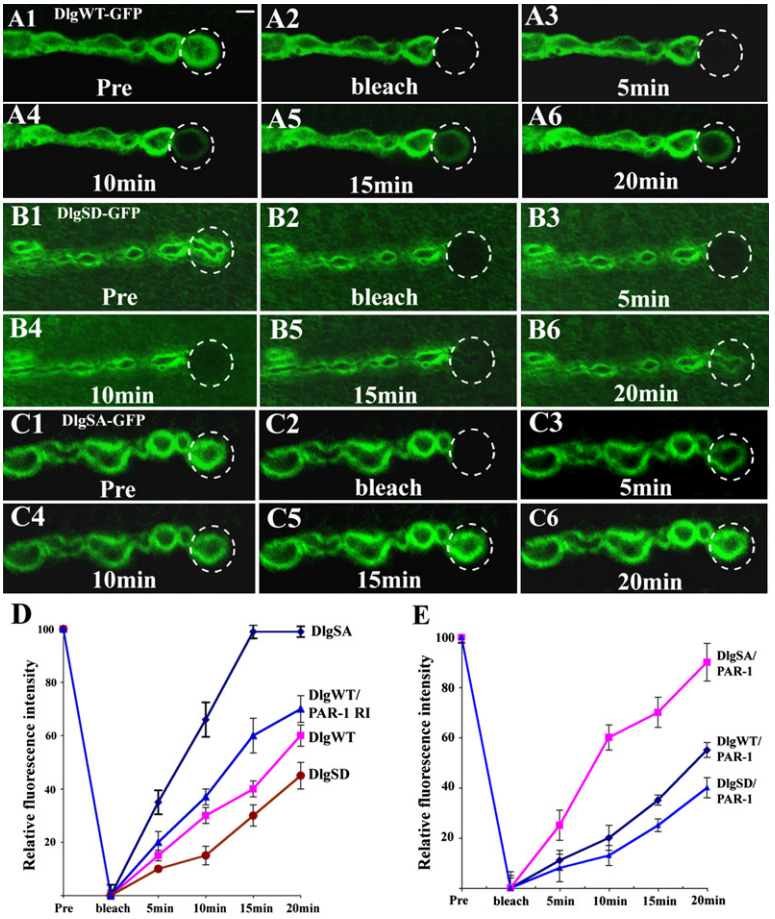

Figure 5. FRAP Analysis of the In Vivo Trafficking Behavior of the Dlg-GFP Variants

(A1–C6) Transgenic third-instar larvae expressing DlgWT-GFP (A1–A6), DlgSD-GFP (B1–B6), or DlgSA-GFP (C1–C6) in a dlg^{X1-2} mutant background were subjected to photobleaching, and the recovery of GFP signal was recorded by confocal microscopy. Images were collected before photobleaching (Pre), immediately after photobleaching (bleach), and every five minutes after photobleaching. The FRAP experiments were repeated at least three times and representative images were chosen. Scale bar in (A1), 2 μm.

(D) The time course of GFP recovery for the three Dlg-GFP variants in a wild-type background and DlgWT-GFP in a *PAR-1 RNAi* background. *Mhc>DlgWT-GFP*, n = 15; *Mhc>DlgSA-GFP*, n = 12; *Mhc>DlgSD-GFP*, n = 14; *Mhc>DlgWT-GFP/PAR-1 RNAi*, n = 17. The differences in fluorescence recovery among the four genotypes at each time point are statistically significant ($p < 0.01$).

(E) The time course of GFP recovery for the three Dlg-GFP variants in a *Mhc>PAR-1* overexpression background. *Mhc>PAR-1/DlgWT-GFP*, n = 16; *Mhc>PAR-1/DlgSA-GFP*, n = 13, and *Mhc>PAR-1/DlgSD-GFP*, n = 11. The differences in fluorescence recovery between *Mhc>PAR-1/DlgWT-GFP* and *Mhc>DlgWT-GFP* at each time point are statistically significant ($p < 0.05$). The recovery of DlgSA-GFP and DlgSD-GFP also showed a trend of reduction in the *Mhc>PAR-1* background compared with that in a wild-type background, but the difference was not statistically significant.

signal from the distal synapse, it took 20 min to achieve a partial (~60%) recovery of GFP signal (Figures 5A and 5D). In contrast, it took less than 10 min for synaptic DlgSA-GFP signal to achieve 60% recovery and ~15 min for 100% recovery (Figures 5B and 5D). DlgSD-GFP recovered more slowly than DlgWT-GFP. For example, DlgWT-GFP achieved approximately 30% recovery after 10 min, whereas DlgSD-GFP only recovered by ~17% in the same period (Figures 5C and 5D). Furthermore, in a *PAR-1 RNAi* background, DlgWT-GFP recovered significantly faster than it did in a wild-type background (Figure 5D). Conversely, in the PAR-1 overexpression background, DlgWT-GFP recovery was reduced compared with that in a wild-type background (Figure 5E). These results further strengthen the notion that phosphorylation of Dlg at S797 negatively regulates its synaptic targeting.

In principle, the recovered GFP signal could come from two sources: (1) Dlg-GFP diffusing from neighboring boutons, where it is already present at the postsynapse; or (2) Dlg-GFP recruited from the extrasynaptic region (muscle cytoplasm). Since in all the FRAP experiments, the GFP intensity in the adjacent boutons didn't show obvious change during the course of recovery, and since we did not see movement of the edges of the bleached regions, the recovered Dlg-GFP signals most likely came from the extrasynaptic region.

DlgSA-GFP, but Not DlgSD-GFP, Can Largely Rescue the Synapse Formation Defects Caused by Postsynaptic PAR-1 Overexpression

We next tested whether Dlg is a key target through which PAR-1 regulates synapse development. DlgWT-, DlgSA-, and DlgSD-GFP were used to rescue the synapse formation defects caused by postsynaptic PAR-1 overexpression. DlgSA-GFP exhibited the most potent rescuing ability. It restored synapse formation to roughly 80% of wild-type level (Figures 6B2 and 6D). DlgWT-GFP showed a lesser rescuing ability than DlgSA-GFP (Figures 6A2 and 6D), whereas DlgSD-GFP was not effective in rescuing the phenotype (Figures 6C2 and 6D). No obvious effect on synapse formation was observed when DlgWT-, DlgSA-, or DlgSD-GFP was expressed in a wild-type background (data not shown). Noticeably, in *Mhc>PAR-1/DlgSD-GFP* animals, a significant portion of GFP fusion protein (~40%) was mislocalized to the muscle cytoplasm (Figure 6E). In contrast, in *Mhc>PAR-1/DlgSA-GFP* animals, the majority of GFP fusion protein was still concentrated at the postsynapse (Figure 6E), indicating that it was resistant to PAR-1-induced delocalization.

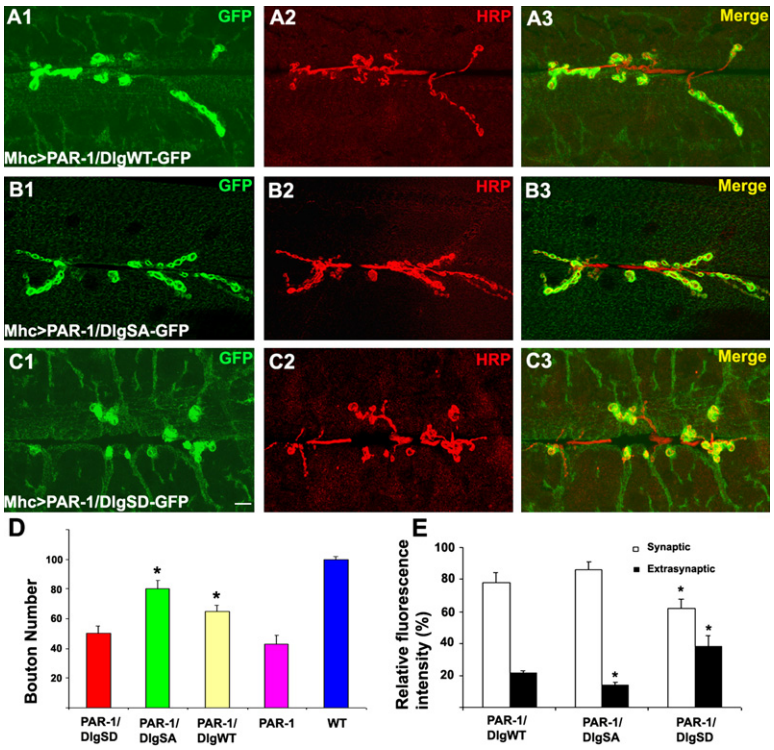

Figure 6. The Nonphosphorylatable DlgSA-GFP Can Largely Rescue the Synapse Formation Defects Caused by PAR-1 Overexpression

(A1–C3) Double-labeling of the NMJs of *Mhc>PAR-1* transgenic animals coexpressing DlgWT-GFP (A1–A3), DlgSA-GFP (B1–B3), or DlgSD-GFP (C1–C3) using anti-GFP (green) and anti-HRP (red). Merged images are shown on the left. Scale bar in (C1), 5 μm.

(D) Quantification of bouton number in *Mhc>PAR-1/DlgWT-GFP* (n = 27), *Mhc>PAR-1/DlgSA-GFP* (n = 30), and *Mhc>PAR-1/DlgSD-GFP* (n = 31). The differences between *Mhc>PAR-1* and *Mhc>PAR-1/DlgSA-GFP* ($p < 0.001$), and between *Mhc>PAR-1* and *Mhc>PAR-1/DlgWT-GFP* ($p < 0.001$), are statistically significant.

(E) Quantification of relative GFP fluorescence intensities between the synaptic and extrasynaptic regions in *Mhc>PAR-1/DlgWT-GFP* (n = 27), *Mhc>PAR-1/DlgSA-GFP* (n = 30), and *Mhc>PAR-1/DlgSD-GFP* (n = 31). The differences in both synaptic and extrasynaptic GFP intensities between *Mhc>PAR-1/DlgSD-GFP* and *Mhc>PAR-1/DlgWT-GFP* ($p < 0.001$) are statistically significant. The difference in extrasynaptic GFP intensity between *Mhc>PAR-1/DlgSA-GFP* and *Mhc>PAR-1/DlgWT-GFP* is statistically significant ($p < 0.01$).

In *Mhc>PAR-1/DlgWT-GFP* animals, the extent of synaptic targeting of GFP signals was less than in *Mhc>DlgWT-GFP* (Figure 4G) or *Mhc>PAR-1/DlgSA-GFP* animals (Figure 6E), indicating that some DlgWT-GFP proteins were delocalized by PAR-1. As an internal control, we examined the relative distribution of GluRIIA in the above genotypes. GluRIIA was predominantly localized to the postsynapse for all the genotypes (Figure S6). Collectively, these results support that Dlg is a primary synaptic target of PAR-1 at the NMJ. Nonetheless, we cannot exclude the possibility that other synaptic targets of PAR-1 may also exist, since even DlgSA-GFP cannot completely rescue the synaptic defects caused by PAR-1 overexpression.

To further prove that Dlg mislocalization is a direct consequence of PAR-1 phosphorylation rather than a secondary event of synaptic structural damages, we examined the localization of endogenous Dlg in *Mhc>PAR-1/DlgSA-GFP* animals. The presence of DlgSA-GFP maintained normal synaptic structures despite the presence of overexpressed PAR-1. However, endogenous Dlg was still mislocalized to the muscle cytoplasm due to PAR-1 overexpression (Figure S9). This argues that the mislocalization of Dlg is a primary effect of phosphorylation by PAR-1.

PAR-1 Loss of Function or Overexpression Leads to Abnormal Synaptic Ultrastructures

Previous studies have revealed remarkable synaptic homeostasis regulation at the *Drosophila* NMJ. When synaptic structure or function is experimentally altered, neurons have the ability to restore their synaptic efficacy back to the normal range (Davis and Goodman, 1998). To gain further insights into the role of PAR-1 in regulating synaptic structure and function, and to test whether synaptic homeostasis is affected by PAR-1, we performed electron microscopy (EM) and electrophysiological analyses. We first examined synaptic ultrastructures of type I boutons formed on muscle 6/7 in *Mhc>PAR-1*, *Mhc>PAR-1 KD*, and *par-1* mutant animals. In *par-1* mutants, the subsynaptic reticulum (SSR), a multifolded membranous structure at the postsynapse, was expanded, and the overall SSR versus bouton area ratio was higher than that of the controls (Figures 7A and 7B and Figure S10), suggesting that loss of PAR-1 enhanced postsynaptic SSR growth. Consistent with this, overgrowth of SSR structures was also observed in *Mhc>PAR-1 RNAi* animals (Figure S10). The SSR overgrowth phenotype was also observed when Dlg was postsynaptically overexpressed (Figure 7E and Figure S10). In contrast, there was a dramatic loss of SSR in *Mhc>PAR-1* animals (Figure 7C and Figure S10). In addition, the presynaptic regions exhibited a moderate decrease in synaptic vesicle density and active zone number in *Mhc>PAR-1* animals (Figure 7C and Figure S10). In dlg^{X1-2} mutant (Figure 7D and Figure S10), the overall SSR structure was also less developed as compared with that of the controls. However, the extent of SSR loss in dlg^{X1-2} mutant was smaller than that in *Mhc>PAR-1* animals, suggesting that elevation of PAR-1 activity and loss of Dlg may have some differential effects on postsynaptic SSR assembly. Loss of PAR-1 or overexpression of Dlg therefore enhanced SSR

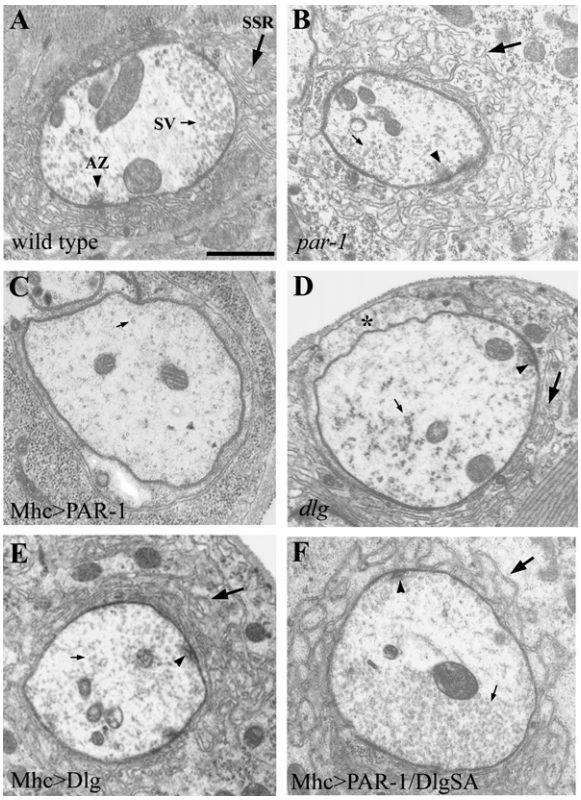

Figure 7. Altered PAR-1 Activities Lead to Aberrant Synaptic Ultrastructures

Electron micrographs of neuromuscular synapses from wild-type (A), *par-1*^{9A}/*par-1*$^{\Delta 16}$ (B), *Mhc>PAR-1* (C), *dlg*$^{X1-2}$ mutant (D), *Mhc>Dlg* (E), and *Mhc>PAR-1/DlgSA-GFP* (F) animals. The SSR, active zone (AZ), and synaptic vesicles (SV) are marked by big arrow, arrowhead, and small arrow, respectively. The asterisk in (D) marks an area of the postsynapse facing the muscle surface that has less SSR layers. Note that in the *par-1* mutant, the SSR area was expanded relative to its bouton area (B). Similar phenotypes were also found in *Mhc>Dlg* (E). However, in *Mhc>PAR-1*, the bouton exhibited a severe loss of SSR (C). The *dlg*$^{X1-2}$ mutant also exhibited a mild loss of SSR (D). The loss of SSR in *Mhc>PAR-1* could be largely restored by DlgSA-GFP (F). Scale bar in (A), 1000 nm.

growth, whereas overexpression of PAR-1 or loss of Dlg had the opposite effect.

To test whether the synaptic ultrastructural defects in *Mhc>PAR-1* animals were due to Dlg dysfunction, we tested the rescuing abilities of DlgWT-, DlgSA-, and DlgSD-GFP. EM morphometric analysis showed that DlgSA-GFP could largely restore SSR growth as well as synaptic vesicle density and active zone number to wild-type levels (Figure 7F and Figure S10). DlgWT-GFP showed less but significant rescue, but DlgSD-GFP failed to do so (Figure S10).

Loss of Function and Overexpression of PAR-1 Affect Synaptic Transmission

To investigate the normal physiological function of PAR-1 at the synapse and the consequence of PAR-1-induced Dlg mislocalization on synaptic transmission, we performed electrophysiological analysis of *par-1* loss-of-function and overexpression animals. Under resting conditions, the frequency and amplitude of miniature excitatory junctional current (mEJC) in *Mhc>PAR-1* animals was reduced by 60% and 40%, respectively, compared with that of the controls (Figures 8A and 8C). In *dlg*$^{X1-2}$ mutant, mEJC amplitude was also reduced, but the frequency was not significantly changed (Figure 8C). In *par-1* mutants, there was a slight increase in mEJC frequency, while the mEJC amplitude was not significantly changed (Figures 8A and 8C). Under stimulated conditions, the amplitude of evoked junctional currents (EJC) was reduced by 44% in *Mhc>PAR-1* animals (Figures 8B and 8C). Despite the changes in mEJC and EJC amplitudes, synaptic junction efficacy represented by quantal content was not significantly altered (Figure 8C), suggesting that some aspect of the synaptic homeostatic mechanism is operating in *Mhc>PAR-1* animals. A similar degree of reduction of EJC amplitude was also observed in *dlg*$^{X1-2}$ mutant (Figure 8C). In contrast, in *par-1* mutants, as well as in *Mhc>PAR-1 KD* animals, EJC amplitude was increased by an estimated 44% (Figures 8B and 8C). Thus, PAR-1 overactivation or Dlg loss-of-function reduced EJC amplitude, whereas loss of PAR-1 had the opposite effect.

We then tested the abilities of the three Dlg-GFP variants to rescue the synaptic transmission defects in *Mhc>PAR-1* animals. DlgWT-GFP and DlgSA-GFP were able to almost fully rescue the mEJC amplitude and frequency defects caused by PAR-1 overexpression. With regard to EJC amplitude in the *Mhc>PAR-1* background, DlgWT-GFP restored it to control level, whereas DlgSA-GFP caused a mild enhancement (Figure 8C), although expression of DlgSA-GFP alone had no significant effect (Figure S11). DlgSA-GFP also caused a moderate increase of quantal content in the *Mhc>PAR-1* background (Figure 8C). In contrast to DlgWT- and DlgSA-GFP, DlgSD-GFP was unable to rescue any of the electrophysiological effects caused by PAR-1 overexpression (Figure 8C). These data, in combination with the morphological rescue data, support our conclusion that PAR-1-induced synaptic defects at the NMJ are primarily caused by Dlg dysfunction.

DISCUSSION

Rearrangement of synaptic protein composition and structure is a fundamental mechanism governing synaptic plasticity. As organizers of the postsynapse, PSD-95/Dlg proteins have been intensively studied as substrates mediating synaptic plasticity. The signaling pathways that couple internal or external cues to the localization and function of PSD-95/Dlg are not well defined. We have found that PAR-1 kinase plays a critical role in regulating the postsynaptic targeting of Dlg at the *Drosophila* NMJ. PAR-1 does so by phosphorylating Dlg at a Ser residue

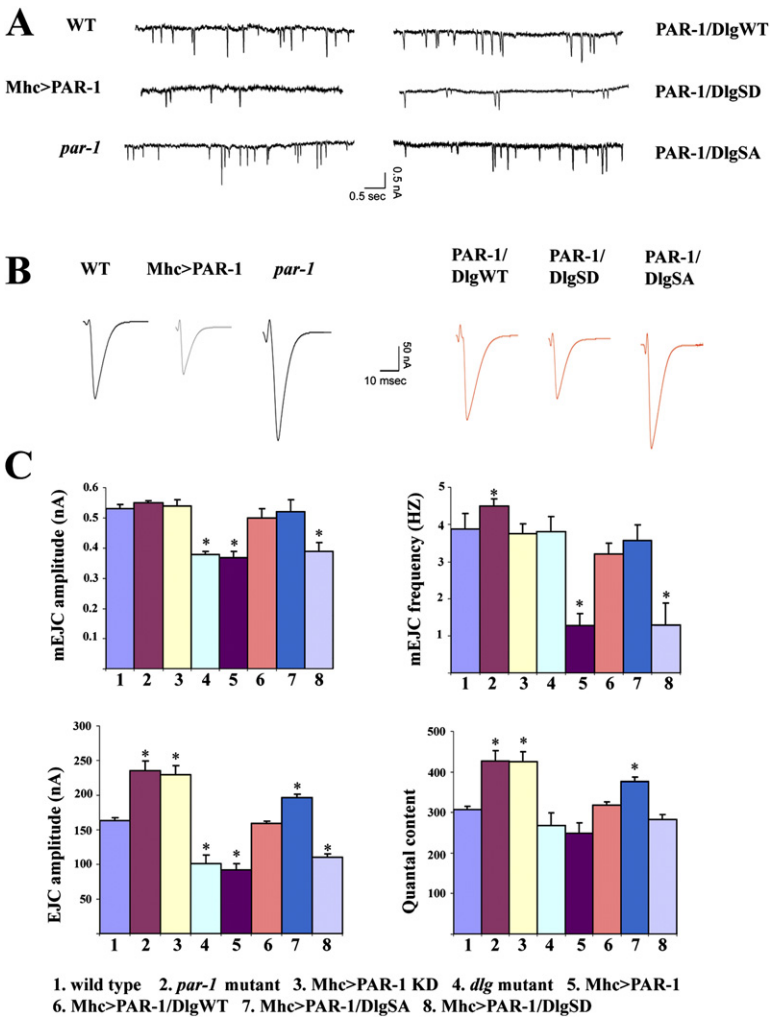

Figure 8. Effects on Synaptic Transmission due to Altered PAR-1 Activities and due to Genetic Interaction between PAR-1 and Dlg

(A) Representative spontaneous release traces showing amplitude and frequency of mEJC in wild-type, *par-1^{9A}/par-1$^{\Delta 16}$* mutant, *Mhc>PAR-1*, *Mhc>PAR-1/DlgWT-GFP*, *Mhc>PAR-1/DlgSA-GFP*, and *Mhc>PAR-1/DlgSD-GFP* NMJs. mEJC amplitude and frequency were both reduced in *Mhc>PAR-1* animals. The mEJC amplitude was normal, but the frequency showed a slight but significant increase in *par-1^{9A}/par-1$^{\Delta 16}$* mutant. DlgSA-GFP and DlgWT-GFP rescued the decreased mEJC frequency and amplitude phenotypes caused by PAR-1 overexpression to differing extents, whereas DlgSD-GFP was unable to do so.

(B) Representative evoked release traces showing amplitude and frequency of EJC in the genotypes mentioned in (A). *par-1^{9A}/par-1$^{\Delta 16}$* mutants showed enhanced EJC amplitude, whereas PAR-1 overexpression animals showed decreased EJC amplitude. DlgSA-GFP and DlgWT-GFP rescued the decreased EJC phenotype caused by PAR-1 overexpression to different degrees, while DlgSD-GFP had no effect.

(C) Bar graphs showing quantitative analysis of mEJC amplitude, mEJC frequency, EJC amplitude, and quantal content in wild-type (n = 30), *par-1^{9A}/par-1$^{\Delta 16}$* mutant (n = 36), *Mhc>PAR-1 KD* (n = 33), *dlg^{X1-2}* mutant (n = 28), *Mhc>PAR-1* (n = 35), *Mhc>PAR-1/DlgWT-GFP* (n = 32), *Mhc>PAR-1/DlgSA-GFP* (n = 35), and *Mhc>PAR-1/DlgSD-GFP* (n = 36) animals. Compared with wild-type, the EJC amplitude and quantal content were increased in *par-1* mutant and *Mhc>PAR-1 KD* animals ($p < 0.01$). In addition, mEJC frequency was slightly increased in *par-1* mutant ($p < 0.05$). In contrast, the mEJC and EJC amplitudes were decreased in *Mhc>PAR-1* animals and *dlg* mutant ($p < 0.01$). In addition, the mEJC frequency was also reduced in *Mhc>PAR-1* ($p < 0.01$). DlgWT-GFP and DlgSA-GFP restored the mEJC amplitude and frequency to normal in *Mhc>PAR-1* background. DlgWT-GFP also restored EJC amplitude to normal, whereas DlgSA-GFP moderately enhanced EJC amplitude and quantal content ($p < 0.05$). DlgSD-GFP had no effect on *Mhc>PAR-1* synaptic transmission defects.

in the GUK domain. The conservation of this Ser residue in all members of the MAGUK proteins suggests that this phosphorylation event may represent a general mechanism by which the MAGUK proteins are regulated. To our knowledge, this is the first time the PAR-1 family of Ser/Thr kinase has been shown to play an important role in synaptic development and function.

PAR-1 Regulates the Dynamic Trafficking of Dlg between the Extrasynaptic and Synaptic Compartments

We have found that PAR-1 directly phosphorylates Dlg and that overactivation of PAR-1 disrupts Dlg's postsynaptic targeting. The physiological function of PAR-1 in regulating Dlg synaptic targeting is supported by loss-of-function analysis, which indicates that phosphorylation by PAR-1 negatively regulates Dlg synaptic targeting. Consistent with this, our in vivo FRAP analysis shows that the nonphosphorylatable DlgSA-GFP recovers much faster than DlgWT-GFP, and that the recovery of DlgWT-GFP is facilitated by PAR-1 loss-of-function, but impeded by PAR-1 overexpression. At first glance, it may seem somewhat counterintuitive that DlgSA-GFP, which accumulates to a greater degree at the synapse than DlgWT-GFP does, is replaced more quickly and to a greater extent that DlgWT-GFP. Since our FRAP analysis suggested that the recovered Dlg comes primarily from Dlg protein reserved or newly synthesized in the muscle cytoplasm rather than from diffusion of Dlg protein from the neighboring synapses, the most likely explanation is that PAR-1-mediated phosphorylation regulates the transport of Dlg from the extrasynaptic to the synaptic regions. DlgSA-GFP may be transported more efficiently from the extrasynaptic region to the postsynapse. Upon reaching the

postsynapse, DlgSA-GFP may also associate with the synaptic membrane more tightly.

Previous studies have demonstrated that the GUK domain, in which the S797 residue is located, plays an important role in the trafficking and synaptic targeting of Dlg (Thomas et al., 2000). The importance of the GUK domain in mediating Dlg function is also highlighted by the fact that many of the identified *dlg* mutations are clustered in this domain (Woods et al., 1996). Two types of protein-protein interactions involving the GUK domain have been previously detected: (1) intramolecular interaction with the SH3 domain (McGee and Bredt, 1999; Shin et al., 2000); and (2) protein-protein interactions with GUK binding proteins, including an MT binding protein and a kinesin motor (Brenman et al., 1998; Hanada et al., 2000; Kim et al., 1997). Since MT and MT-based motor proteins provide a major driving force for protein and mRNA trafficking, it is possible that PAR-1-mediated phosphorylation may regulate Dlg interaction with the MT-based transport system.

Dlg Is a Primary Postsynaptic Target of PAR-1

Our morphological and electrophysiological rescue experiments strongly support that Dlg is a critical downstream target through which PAR-1 impacts synapse differentiation and function. However, the rescue of PAR-1 overexpression-induced defects by DlgSA-GFP is not complete, raising the possibility that other synaptic substrates are affected by PAR-1. It is also possible that some of the PAR-1 overexpression phenotypes are neomorphic. A possible neomorphic effect caused by the synaptic upregulation of a kinase was recently described (Collins et al., 2006). None of the known postsynaptic markers, such as CaMKII, FasII, or GluRIIA has the KXGS motif, suggesting that they may not be PAR-1 targets. In other developmental contexts, PAR-1/MARK kinases phosphorylate a number of substrates (Drewes, 2004). Whether any of these PAR-1 substrates function at the synapse awaits further investigation. The existence of other synaptic targets of PAR-1 could also explain why we were unable to effectively rescue *par-1* mutant phenotypes with the Dlg-GFP variants (data not shown), although there are other possible explanations for this result. For example, phosphorylated Dlg may possess certain biological activity that cannot be provided by DlgSD-GFP. Even if some of the phenotypes caused by altered PAR-1 activities are mediated by other substrates, several lines of evidence indicate that the mislocalization of Dlg is a primary effect of PAR-1 phosphorylation of Dlg, rather than a secondary consequence of synaptic damages caused by PAR-1 action on some unknown target(s). First, the phospho-mimetic DlgSD-GFP is mislocalized in a wild-type background, in the presence of normal synaptic structures. Second, another postsynaptic marker, GluRIIA, retains its predominant postsynaptic localization in a PAR-1 overexpression situation. Third, we could largely rescue the SSR loss and synaptic transmission defects caused by PAR-1 overexpression using DlgSA-GFP. Finally, in a condition where postsynaptic structure was maintained with exogenous DlgSA-GFP, endogenous Dlg was still mislocalized in the presence of overexpressed PAR-1 (Figure S9).

Recent studies suggest that posttranslational modification plays a role in regulating the trafficking of PSD-95/Dlg. In mammalian central synapses, N-terminal palmitoylation is critical for the intracellular sorting, postsynaptic targeting, and surface expression of PSD-95 (Chetkovich et al., 2002; Craven et al., 1999; El-Husseini et al., 2000). Cyclin-dependent kinase 5 (Cdk5) phosphorylates the N-terminal region of PSD-95, inhibiting its oligomerization, channel clustering activity, and possibly, synaptic localization (Morabito et al., 2004). Our study establishes PAR-1-mediated phosphorylation at the C-terminal GUK domain as a regulatory mechanism in the synaptic targeting of Dlg. In addition, two independent studies have been conducted to study the function of CaMKII at the *Drosophila* NMJ. However, divergent results were obtained on the effect of CaMKII on synaptic development and function, and it appears that further studies are needed to clarify the function of CaMKII at the *Drosophila* NMJ (Haghighi et al., 2003; Koh et al., 1999). Future studies of upstream signaling events in the regulation of PAR-1 at the synapse, especially those which potentially regulate the PAR-1-Dlg phosphorylation cascade, will provide new insights on molecular mechanisms that regulate synaptic differentiation and plasticity.

PAR-1 and Dlg Affect both Pre- and Postsynaptic Development and Function

It is interesting to note that in addition to postsynaptic defects, altering PAR-1 activity leads to profound defects in presynaptic development and function. This indicates that PAR-1 regulates the coordinated maturation of pre- and postsynaptic structures. PAR-1 could regulate the adhesion between the pre- and postsynaptic membranes or *trans*-synaptic signaling. Intriguingly, a previous study has revealed a presynaptic localization and function for Dlg in regulating neurotransmission (Budnik et al., 1996). Since a fraction of PAR-1 is localized at the presynapse, it raises the possibility that PAR-1 may also play a role there. Further studies are needed to test whether PAR-1 may act through Dlg or other substrates at the presynapse to affect neurotransmission. Previous studies have also implicated BMP as a retrograde signal that modulates presynaptic development and function in response to postsynaptic alterations (McCabe et al., 2003). It would be interesting to explore the relationship between PAR-1 and Dlg-mediated synaptic effects and BMP-mediated retrograde signaling.

Our current model predicts that PAR-1 overactivation causes Dlg hyperphosphorylation and delocalization from the synapse, producing certain Dlg loss-of-function effects. On the other hand, loss of PAR-1 function has the opposite effect, causing Dlg overactivation phenotypes. Most of the phenotypes we observe are consistent with this model. For example, at the morphological level,

PAR-1 overexpression and Dlg inactivation both lead to SSR loss, whereas loss of PAR-1 and overexpression of Dlg promote SSR growth. At the electrophysiological level, PAR-1 overexpression or Dlg loss of function leads to reduced EJC amplitude, whereas loss of PAR-1 has the opposite effect. The genetic interaction between PAR-1 and Dlg is also consistent with an antagonistic effect of PAR-1 on Dlg. We also note some inconsistencies of certain PAR-1 overexpression phenotypes and previously published *dlg* mutant phenotypes. For example, overexpression of PAR-1 in the postsynapse causes reductions in both active zone number and synaptic vesicle density, whereas quite variable phenotypes, ranging from no obvious structural alteration in the presynapse to reduction in synaptic vesicle density or increase in active zone number, were described for different *dlg* mutant alleles (Budnik et al., 1996; Lahey et al., 1994; Thomas et al., 1997). Similarly, in electrophysiological studies, we found a decrease in both mEJC and EJC amplitudes, but no significant change in quantal content, in both *Mhc>PAR-1* animals and dlg^{X1-2} mutants. These neurotransmission phenotypes are different from those previously reported for *dlg* mutant alleles dlg^{m52} and dlg^{v59}, in which EJC was increased, whereas mEJC was not changed (Budnik et al., 1996). However, a recent study also reported features of reduced neurotransmission in dlg^{X1-2} mutant (Chen and Featherstone, 2005). It is therefore possible that different *dlg* mutant alleles may differentially affect synaptic function.

Implications for Neurodegenerative Diseases

Recent studies have revealed a tight correlation between synaptic dysfunction and the pathogenesis of neurodegenerative diseases and other neurological disorders. In AD in particular, synaptic dysfunction occurs decades before the onset of amyloid plaque and neurofibrillary tangle formation and discernable neuronal loss (Selkoe, 2002). Intriguingly, loss of PSD-95 protein has been observed in AD patients (Gylys et al., 2004). It is conceivable that under disease conditions, an increase of PAR-1/MARK activity might occur in response to certain neurotoxic insults, leading to abnormal phosphorylation and delocalization of PSD-95 from the postsynapse, eventually leading to neuronal dysfunction and death. Further studies in human AD postmortem tissues and mouse AD models will test the potential role of PAR-1/MARK kinases in regulating PSD-95 function and disease pathogenesis.

EXPERIMENTAL PROCEDURES

See Supplemental Experimental Procedures for detailed methods on Immunocytochemistry, Electrophysiology, Electron Microscopy, and FRAP.

Fly Strains

The $par\text{-}1^{9A}$ and $par\text{-}1^{W3}$ mutants were obtained from Dr. Anne Ephrussi (Tomancak et al., 2000) and Dr. Daniel St. Johnston (Shulman et al., 2000), respectively; the $par\text{-}1^{\Delta 16}$ null allele was described before (Sun et al., 2001); the dlg^{X1-2} mutant was provided by Dr. Peter Bryant (Woods and Bryant, 1991); the *UAS-PAR-1-GFP* flies were provided by Dr. Daniel St. Johnston (Doerflinger et al., 2006); the *Mhc-Gal4* driver was obtained from Dr. Troy Littleton; and *elav-Gal4* was obtained from Bloomington *Drosophila* Stock Center. The *UAS-DlgWT-GFP*, *UAS-DlgSA-GFP*, and *UAS-DlgSD-GFP* transgenics were generated using standard germline transformation. Transgenic lines expressing comparable levels of Dlg-GFP were chosen for further analysis. *PAR-1 RNAi* flies were generated by germline transformation with a *UAS-PAR-1 RNAi* construct containing a *par-1* genomic DNA-cDNA hybrid.

Molecular Biology

The *dlg* S97 cDNA was a gift from Dr. Ulrich Thomas (Thomas et al., 2000). Site-directed mutagenesis at S797 was performed as described before (Nishimura et al., 2004). After confirming the conversion of Ser residue into either Ala or Asp residue by sequencing, the *DlgWT-GFP*, *DlgSA-GFP*, and *DlgSD-GFP* cDNA inserts were ligated into *pUAST* vector for germline transformation. See Supplemental Experimental Procedures for the construction of *UAS-PAR-1 RNAi.*

Electron Microscopy

Electron microcopy analysis was performed essentially as described (Lahey et al., 1994). See Supplemental Experimental Procedures for details.

Electrophysiology

Electrophysiological recordings of two-electrode voltage-clamp were performed as described (Guo and Zhong, 2006). See Supplemental Experimental Procedures for details.

Supplemental Data

The Supplemental Data for this article can be found online at http://www.neuron.org/cgi/content/full/53/2/201/DC1/.

ACKNOWLEDGMENTS

We are grateful to Dr. Isao Nishimura for initial insights on PAR-1 function at the synapse; Dr. Tian-Qiang Sun for the gift of PAR-1 antibody; Drs. Anne Ephrussi, Daniel St. Johnston, Peter Bryant, Troy Littleton, Ulrich Thomas, and the Bloomington Stock Center for fly stocks and cDNA; Jian Hong for technical assistance in the EM experiments; and Larry Ackerman for advice on FRAP. We thank Dr. Su Guo for reading the manuscript and members of the Lu laboratory for discussions and help. Supported by the McKnight Scholar Award, the Beckman Foundation Young Investigator Award, and NIH grant NS043167 (B.L.).

Received: June 29, 2006
Revised: November 8, 2006
Accepted: December 14, 2006
Published: January 17, 2007

REFERENCES

Augustinack, J.C., Schneider, A., Mandelkow, E.M., and Hyman, B.T. (2002). Specific tau phosphorylation sites correlate with severity of neuronal cytopathology in Alzheimer's disease. Acta Neuropathol. (Berl.) *103*, 26–35.

Biernat, J., Wu, Y.Z., Timm, T., Zheng-Fischhofer, Q., Mandelkow, E., Meijer, L., and Mandelkow, E.M. (2002). Protein kinase MARK/PAR-1 is required for neurite outgrowth and establishment of neuronal polarity. Mol. Biol. Cell *13*, 4013–4028.

Brenman, J.E., Topinka, J.R., Cooper, E.C., McGee, A.W., Rosen, J., Milroy, T., Ralston, H.J., and Bredt, D.S. (1998). Localization of postsynaptic density-93 to dendritic microtubules and interaction with microtubule-associated protein 1A. J. Neurosci. *18*, 8805–8813.

Budnik, V., Koh, Y.H., Guan, B., Hartmann, B., Hough, C., Woods, D., and Gorczyca, M. (1996). Regulation of synapse structure and function by the Drosophila tumor suppressor gene dlg. Neuron *17*, 627–640.

Chen, K., and Featherstone, D.E. (2005). Discs-large (DLG) is clustered by presynaptic innervation and regulates postsynaptic glutamate receptor subunit composition in Drosophila. BMC Biol. *3*, 1.

Chetkovich, D.M., Bunn, R.C., Kuo, S.H., Kawasaki, Y., Kohwi, M., and Bredt, D.S. (2002). Postsynaptic targeting of alternative postsynaptic density-95 isoforms by distinct mechanisms. J. Neurosci. *22*, 6415–6425.

Collins, C.A., Wairkar, Y.P., Johnson, S.L., and DiAntonio, A. (2006). Highwire restrains synaptic growth by attenuating a MAP kinase signal. Neuron *51*, 57–69.

Craven, S.E., El-Husseini, A.E., and Bredt, D.S. (1999). Synaptic targeting of the postsynaptic density protein PSD-95 mediated by lipid and protein motifs. Neuron *22*, 497–509.

Davis, G.W., and Goodman, C.S. (1998). Genetic analysis of synaptic development and plasticity: homeostatic regulation of synaptic efficacy. Curr. Opin. Neurobiol. *8*, 149–156.

Davis, G.W., Schuster, C.M., and Goodman, C.S. (1997). Genetic analysis of the mechanisms controlling target selection: target-derived Fasciclin II regulates the pattern of synapse formation. Neuron *19*, 561–573.

DiAntonio, A., Petersen, S.A., Heckmann, M., and Goodman, C.S. (1999). Glutamate receptor expression regulates quantal size and quantal content at the Drosophila neuromuscular junction. J. Neurosci. *19*, 3023–3032.

Doerflinger, H., Benton, R., Torres, I.L., Zwart, M.F., and St Johnston, D. (2006). Drosophila anterior-posterior polarity requires actin-dependent PAR-1 recruitment to the oocyte posterior. Curr. Biol. *16*, 1090–1095.

Drewes, G. (2004). MARKing tau for tangles and toxicity. Trends Biochem. Sci. *29*, 548–555.

Drewes, G., Ebneth, A., Preuss, U., Mandelkow, E.M., and Mandelkow, E. (1997). MARK, a novel family of protein kinases that phosphorylate microtubule-associated proteins and trigger microtubule disruption. Cell *89*, 297–308.

El-Husseini, A.E., Craven, S.E., Chetkovich, D.M., Firestein, B.L., Schnell, E., Aoki, C., and Bredt, D.S. (2000). Dual palmitoylation of PSD-95 mediates its vesiculotubular sorting, postsynaptic targeting, and ion channel clustering. J. Cell Biol. *148*, 159–172.

Funke, L., Dakoji, S., and Bredt, D.S. (2005). Membrane-associated guanylate kinases regulate adhesion and plasticity at cell junctions. Annu. Rev. Biochem. *74*, 219–245.

Goda, Y., and Davis, G.W. (2003). Mechanisms of synapse assembly and disassembly. Neuron *40*, 243–264.

Guo, H.F., and Zhong, Y. (2006). Requirement of Akt to mediate long-term synaptic depression in Drosophila. J. Neurosci. *26*, 4004–4014.

Guo, S., and Kemphues, K.J. (1995). par-1, a gene required for establishing polarity in C. elegans embryos, encodes a putative Ser/Thr kinase that is asymmetrically distributed. Cell *81*, 611–620.

Gylys, K.H., Fein, J.A., Yang, F., Wiley, D.J., Miller, C.A., and Cole, G.M. (2004). Synaptic changes in Alzheimer's disease: increased amyloid-beta and gliosis in surviving terminals is accompanied by decreased PSD-95 fluorescence. Am. J. Pathol. *165*, 1809–1817.

Haghighi, A.P., McCabe, B.D., Fetter, R.D., Palmer, J.E., Hom, S., and Goodman, C.S. (2003). Retrograde control of synaptic transmission by postsynaptic CaMKII at the Drosophila neuromuscular junction. Neuron *39*, 255–267.

Hanada, T., Lin, L., Tibaldi, E.V., Reinherz, E.L., and Chishti, A.H. (2000). GAKIN, a novel kinesin-like protein associates with the human homologue of the Drosophila discs large tumor suppressor in T lymphocytes. J. Biol. Chem. *275*, 28774–28784.

Humbert, P., Russell, S., and Richardson, H. (2003). Dlg, Scribble and Lgl in cell polarity, cell proliferation and cancer. Bioessays *25*, 542–553.

Jan, L.Y., and Jan, Y.N. (1976). L-glutamate as an excitatory transmitter at the Drosophila larval neuromuscular junction. J. Physiol. *262*, 215–236.

Jan, L.Y., and Jan, Y.N. (1982). Antibodies to horseradish peroxidase as specific neuronal markers in Drosophila and in grasshopper embryos. Proc. Natl. Acad. Sci. USA *79*, 2700–2704.

Kemphues, K.J., Priess, J.R., Morton, D.G., and Cheng, N.S. (1988). Identification of genes required for cytoplasmic localization in early C. elegans embryos. Cell *52*, 311–320.

Kennedy, M.J., and Ehlers, M.D. (2006). Organelles and trafficking machinery for postsynaptic plasticity. Annu. Rev. Neurosci. *29*, 325–632. Published online March 20, 2006. 10.1146/annurev.neuro.29.051605.112808.

Kim, E., and Sheng, M. (2004). PDZ domain proteins of synapses. Nat. Rev. Neurosci. *5*, 771–781.

Kim, E., Naisbitt, S., Hsueh, Y.P., Rao, A., Rothschild, A., Craig, A.M., and Sheng, M. (1997). GKAP, a novel synaptic protein that interacts with the guanylate kinase-like domain of the PSD-95/SAP90 family of channel clustering molecules. J. Cell Biol. *136*, 669–678.

Koh, Y.H., Popova, E., Thomas, U., Griffith, L.C., and Budnik, V. (1999). Regulation of DLG localization at synapses by CaMKII-dependent phosphorylation. Cell *98*, 353–363.

Koh, Y.H., Gramates, L.S., and Budnik, V. (2000). Drosophila larval neuromuscular junction: molecular components and mechanisms underlying synaptic plasticity. Microsc. Res. Tech. *49*, 14–25.

Lahey, T., Gorczyca, M., Jia, X.X., and Budnik, V. (1994). The Drosophila tumor suppressor gene dlg is required for normal synaptic bouton structure. Neuron *13*, 823–835.

Lin, D.M., and Goodman, C.S. (1994). Ectopic and increased expression of Fasciclin II alters motoneuron growth cone guidance. Neuron *13*, 507–523.

Lnenicka, G.A., and Keshishian, H. (2000). Identified motor terminals in Drosophila larvae show distinct differences in morphology and physiology. J. Neurobiol. *43*, 186–197.

McCabe, B.D., Marques, G., Haghighi, A.P., Fetter, R.D., Crotty, M.L., Haerry, T.E., Goodman, C.S., and O'Connor, M.B. (2003). The BMP homolog Gbb provides a retrograde signal that regulates synaptic growth at the Drosophila neuromuscular junction. Neuron *39*, 241–254.

McGee, A.W., and Bredt, D.S. (1999). Identification of an intramolecular interaction between the SH3 and guanylate kinase domains of PSD-95. J. Biol. Chem. *274*, 17431–17436.

Mendoza, C., Olguin, P., Lafferte, G., Thomas, U., Ebitsch, S., Gundelfinger, E.D., Kukuljan, M., and Sierralta, J. (2003). Novel isoforms of Dlg are fundamental for neuronal development in Drosophila. J. Neurosci. *23*, 2093–2101.

Morabito, M.A., Sheng, M., and Tsai, L.H. (2004). Cyclin-dependent kinase 5 phosphorylates the N-terminal domain of the postsynaptic density protein PSD-95 in neurons. J. Neurosci. *24*, 865–876.

Nishimura, I., Yang, Y., and Lu, B. (2004). PAR-1 kinase plays an initiator role in a temporally ordered phosphorylation process that confers tau toxicity in Drosophila. Cell *116*, 671–682.

Parnas, D., Haghighi, A.P., Fetter, R.D., Kim, S.W., and Goodman, C.S. (2001). Regulation of postsynaptic structure and protein localization by the Rho-type guanine nucleotide exchange factor dPix. Neuron *32*, 415–424.

Rasse, T.M., Fouquet, W., Schmid, A., Kittel, R.J., Mertel, S., Sigrist, C.B., Schmidt, M., Guzman, A., Merino, C., Qin, G., et al. (2005). Glutamate receptor dynamics organizing synapse formation in vivo. Nat. Neurosci. *8*, 898–905.

Selkoe, D.J. (2002). Alzheimer's disease is a synaptic failure. Science *298*, 789–791.

Shin, H., Hsueh, Y.P., Yang, F.C., Kim, E., and Sheng, M. (2000). An intramolecular interaction between Src homology 3 domain and guanylate kinase-like domain required for channel clustering by postsynaptic density-95/SAP90. J. Neurosci. *20*, 3580–3587.

Shulman, J.M., Benton, R., and St Johnston, D. (2000). The Drosophila homolog of C. elegans PAR-1 organizes the oocyte cytoskeleton and directs oskar mRNA localization to the posterior pole. Cell *101*, 377–388.

Sun, T.Q., Lu, B., Feng, J.J., Reinhard, C., Jan, Y.N., Fantl, W.J., and Williams, L.T. (2001). PAR-1 is a Dishevelled-associated kinase and a positive regulator of Wnt signalling. Nat. Cell Biol. *3*, 628–636.

Thomas, U., Kim, E., Kuhlendahl, S., Koh, Y.H., Gundelfinger, E.D., Sheng, M., Garner, C.C., and Budnik, V. (1997). Synaptic clustering of the cell adhesion molecule fasciclin II by discs-large and its role in the regulation of presynaptic structure. Neuron *19*, 787–799.

Thomas, U., Ebitsch, S., Gorczyca, M., Koh, Y.H., Hough, C.D., Woods, D., Gundelfinger, E.D., and Budnik, V. (2000). Synaptic targeting and localization of discs-large is a stepwise process controlled by different domains of the protein. Curr. Biol. *10*, 1108–1117.

Tomancak, P., Piano, F., Riechmann, V., Gunsalus, K.C., Kemphues, K.J., and Ephrussi, A. (2000). A Drosophila melanogaster homologue of Caenorhabditis elegans par-1 acts at an early step in embryonic-axis formation. Nat. Cell Biol. *2*, 458–460.

Woods, D.F., and Bryant, P.J. (1991). The discs-large tumor suppressor gene of Drosophila encodes a guanylate kinase homolog localized at septate junctions. Cell *66*, 451–464.

Woods, D.F., Hough, C., Peel, D., Callaini, G., and Bryant, P.J. (1996). Dlg protein is required for junction structure, cell polarity, and proliferation control in Drosophila epithelia. J. Cell Biol. *134*, 1469–1482.

Zinsmaier, K.E., Eberle, K.K., Buchner, E., Walter, N., and Benzer, S. (1994). Paralysis and early death in cysteine string protein mutants of Drosophila. Science *263*, 977–980.

Zito, K., Parnas, D., Fetter, R.D., Isacoff, E.Y., and Goodman, C.S. (1999). Watching a synapse grow: noninvasive confocal imaging of synaptic growth in Drosophila. Neuron *22*, 719–729.